Int. J. Electrochem. Sci., 11 **(2016)** 3786 - 3802

International Journal of ELECTROCHEMICAL SCIENCE
www.electrochemsci.org

Effect of Zeta Potential of Exfoliated Amphiphilic Montmorillonite Nanogels on Removal Efficiencies of Cationic Dye water pollutant

Ayman M. Atta[1,2,*] *, Hamad A. Al-Lohedan*[1]*, Z. A. ALOthman*[3]*, Ahmed M. Tawfeek*[4]*, Ayman AbdelGhafar*[3] *Nora A. Hamad*[5]

[1] Chemistry Department, College of Science, King Saud University, Riyadh , Kingdom of Saudi Arabia
[2] Egyptian Petroleum Research Institute, Nasr City, Cairo 11727, Egypt
[3] Chemistry Department, College of Science, King Saud University, Riyadh , Kingdom of Saudi Arabia
[4] College of Science, King Saud University, Riyadh , Kingdom of Saudi Arabia
[5] Department of Chemistry, Faculty of Science & Arts, Al Jouf University, Qurayyat, Saudi Arabia
[*]E-mail: aatta@ksu.edu.sa

Received: 17 January 2016 / *Accepted:* 19 March 2016 / *Published:* 1 April 2016

The zeta or electrokinetic potential describes the nanomaterials potential distribution and it is often a useful parameter to evaluate the adsorption of ionic pollutants on the nanomaterials surfaces, since it reflects the electrostatic interactions of water pollutants on the nanomaterials surfaces. In this respect, sodium montmorillonite (Na-MM) attracted great attention in the removal of toxic pollutants from water. The present work aims to increase the ability of MMT to act as amphiphiles to increase the diffusion of pollutants into MMT galleries. The exchange of Na cations with a cationic monomer based on 3-acrylamidopropyl trimethylammonium chloride followed by crosslinking copolymerization achieves this goal. Therefore, different MMT copolymer nanogels based on APTAC were prepared using anionic and nonionic co- monomers and characterized by FTIR, TEM, WXD, and zeta potential analyses. The surface activity of the amphiphilic MMT nanogels was evaluated from the surface tension measurements. The adsorption of MB on the surface of Na-MMT was studied at different MMT nanogel concentrations, and pH through zeta potential measurements. The removal efficiencies of MMT nanogels for removing methylene blue as cationic dye from water were measured at room temperature and pH 7. The data indicated that the removal efficiencies of MMT nanogels increased by complete exfoliation of MMT layers and their high surface activity that increased the MB penetration into the network of MMT nanogel.

Keywords: Zeta potential; water pollutants; sodium montmorillonite; adsorption; cationic dye.

doi: 10.20964/110379

1. INTRODUCTION

Nanotechnology plays an important role in the water treatment, desalination and purification [1-3]. Nowadays, nanomaterials have been used for water treatment as nano-fibers, nano-filters and adsorbents [4-6]. There are several pollutants that change the drinking and industrial waste water such as organic, inorganic pollutants and biological substances such as algae [7]. Organic dyes and heavy metals have several toxicity and hazardous problems that have serious health problems, according to US protection agency [8]. Nanomaterials based on inorganic substances such as clay minerals, titanium dioxide, silica, silver and magnetite attracted great attention in the field of water purification to remove organic and inorganic pollutants [9-13]. Moreover, crosslinked organic polymers such as hydrogels, microgels and nanogels achieved good results for the removal of water pollutants [14-17]. The combination between inorganic and organic nanomaterials succeeded to achieve high adsorption for removing of toxic pollutants. Accordingly, there is an emerging need to develop novel low cost and more economic techniques and materials that contains hybrid polymers to remove organic pollutants at low concentration below part per billion (ppb).

There are several clay minerals such as sepiolite, kaolinite, bentonite and montmorlonite are used in the water treatments for the removal of organic and inorganic pollutants [18-20]. The exfoliation of clay minerals using organic and inorganic nanomaterials increases the rate of adsorption of toxic substances from water [21-23]. The techniques used to exfoliate the clay minerals are based on the cationic exchange with cationic surfactants or crosslinking of monomers between clay galleries [24-25]. Moreover, the thermosensitive polymers succeeded to exfoliate clay minerals using 20 % of clay in the polymer composites [26]. In our previous work, sodium montmorillonite (Na-MMT) galleries are exfoliated using anionic nanogels [27-28]. The main difference between the present work and previous researches on the polymer-clay nanocomposites is based on the modification of the surface activity of the clay galleries to increase their removal efficiency for toxic cationic dyes. The zeta potential measurements can be used to determine the variation of surface charges on the electrostatic interaction forces between adsorbents and anionic dyes. Moreover, zeta potential describes the potential distribution on the nanomaterial surfaces. Therefore, the aim of present work is a demonstration of a new approach to synthesize amphiphilic dispersed clay particles having ability to reduce the surface tension of water via zeta potential to increase the diffusion rate of toxic materials to the Na-MMT polymer composites. The cationic monomer based on 3-acrylamidopropyl) trimethylammonium chloride (APTAC) is copolymerized and crosslinked with anionic and nonionic monomers in the presence of crosslinker to exfoliate the clay galleries by forming nanogel composites. The application of the prepared Na-MMT nanogel composites for removal of the cationic methylene blue (MB) dye is another objective of the present work.

2. EXPERIMENTAL

2.1. Materials

Sodium montmorillonite nanoclay (Na-MMT; nanometer PGV obtained from Sigma-Aldrich Co) is used as clay mineral. Cationic monomer of 3-acrylamidopropyl trimethylammonium chloride

solution (APTAC; 75 wt. % in H_2O; Aldrich Chemicals Co.) is used to exchange Na cation from Na-MMT. Nonionic monomers such as N-vinyl pyrrolidone (VP) and acrylamide (AAm) purchased from Aldrich Chemical Co are used to copolymerize with APTAC to investigate the effect of nonionic monomers on intercalation and exfoliation of MMT layers. Ionic monomers such as acrylic acid (AA), sodium 2- acrylamido-2-methylpropane sulfonate (Na-AMPS; 50 wt. % in H_2O; Aldrich Chemicals Co.) and 2- acrylamido-2-methylpropane sulfonic acid (AMPS) are used without further purification. The suspending agent based on poly (vinyl pyrrolidone), PVP; with molecular weight 40000 g/mol, is purchased from Sigma-Aldrich Co. Tetra-functional crosslinking agent of N,N-methylenebisacrylamide (MBA), radical initiator of ammonium persulfate (APS) and activator N,N,N′,N′-tetramethylethylenediamine (TEMED) are used to prepare nanogels at low temperature. Phosphate buffer solutions (PBS) having pH range 2 — 12 are used to study the performance of nanocomposites at different pH solutions.

2.2. Synthesis procedure

The dispersion crosslinking homo-polymerization of APTAC with Na-MMT clay was discussed in previous work [27, 28] using water/ethanol (60/40 vol %) as mixed solvent. So that, Na-MMT (2 g) and APTAC monomer (2 ml) were mixed in water/ethanol (100 mL) and PVP (0.3 g) at room temperature for 24 hrs. AAm (1gm) was dissolved in the MMT/APTAC solution. APS (0.03 g), MBA (0.03 g) and 20 µl TEMED dissolved in water (2 ml) were added to start the polymerization. The reaction temperature was raised to 45 ^oC to complete the polymerization under stirring and nitrogen inlet atmosphere for 24 hrs. The dispersed MMT-APTAC/AAm nanogel solution was separated using ultra-centrifuge at 12000 rpm for 30 minute five times and washed with ethanol and dried under vacuum at 30 ^oC.

The same procedure was used to synthesize MMT nanogels with APTAC/Na-AMPS, APTAC/Na-AMPS, APTAC/AAm and APTAC/AA the mol ratio between APTAC and other monomers was 1:1.

2.3. Characterization:

Fourier transform infrared (FTIR spectrometer; Nicolet, NEXUS-670) was used to confirm the interaction between MMT and nanogels.

Wide-angle X-ray diffraction (WAX; Rigaku D/MAX-3C OD- 2988N X-ray; CuKα radiation; λ= 0.15418 at 40 kV and 30 mA) is a recommended analysis to determine the intercalation and exfoliation of MMT galleries.

Transmittance electron microscope (TEM; JEOL JEM-2100 F has an acceleration voltage of 200 kV) was used to study the nanogel and MMT morphologies.

Thermogravimetric and diffraction thermal analyses (TGA-50 SHIMADZU) were used to study thermal stability and nanogels decomposition temperatures at a heating rate of 10 ^oC/min.

Zeta potentials were determined using Laser Zeta meter Malvern Instruments (Model Zetasizer 2000) in aqueous solution in the presence of KCl (0.01 M) at different pH solutions.

The concentrations of methylene blue dye (MB) in water at different pH solutions were investigated before and after mixing with MMT nanogels using double beam UV/vis spectrophotometer at wavelength of 662 nm.

The surface parameters determined from surface tension measurement in aqueous solution were measured at 25 ^{o}C using drop shape analyzer model DSA-100.

2.4. Adsorption and desorption experiments

Working aqueous solutions of MB (1, 2, 3, 4, 5 ppm) were measured spectrophotometric at a wavelength of 662 nm to establish the standard calibration curve. The absorbance of unknown sample was determined from the standard calibration curve at the same wavelength. Different concentrations of MB (100-1000 ppm) dissolved in 50 ml of PBS and stirred with 0.02 g of the MMT nanogels into a 100 ml conical flask at 25 °C. The filtrate samples were centrifuged and analyzed at different time intervals. The MB concentration was determined at the same wavelength (662 nm). The amount of dye adsorption at equilibrium Q (mg/g) and percent extraction (%E) was calculated from the following equation:

$$Q= [(C_o-C_e)\ xV/(m)] \quad (1)$$

$$\%E= [(C_o-C_e)\ x100/(C_o)] \quad (2)$$

Where C_o and C_e (mg/L) are the liquid phase concentrations of dye at initial and equilibrium, respectively, V (L) the volume of the solution and m (g) is the mass of adsorbent used.

In order to estimate the recovery of MB from MMT nanogels to reuse as adsorbents, desorption experiments were performed using 2 M HNO_3. The acid treated sample was neutralized with 0.1 M NaOH, washed with distilled water and also used for adsorption experiments.

3. RESULTS AND DISCUSSION

Na-MMT clay is strongly hydrated mineral in water due to the presence of Na^+, Ca^{2+} and H^+ cations in internal and external layers of alumina silicate galleries [29, 30]. The conversion of hydrophilic Na-MMT to organic modified clay is very important to increase its adsorption capacity [31]. The balance between hydrophilic and hydrophobic part is very important to determine the adsorption performance and surface properties of clay [32]. The changes in the surface properties of clay affect their performance to apply as adsorbents for toxic pollutants in the water [33]. Caption exchanges are the most effective techniques that can change the clay characteristics with intercalation and exfoliation of clay layers using alkyl ammonium cationic surfactants [34-35]. The ionic surfactants cannot intercalate the clay galleries due to difficult exchange between clay layers. In the present work, the aim is using of APTAC cationic monomer to exchange the Na^+ of MMT layers. The modified organic MMT can copolymerized and crosslinked with ionic monomers (such as AMPS, Na-AMPS

and AA) or nonionic monomers (such as VP and AAm) in the presence of MBA crosslinker as illustrated in Scheme 1.

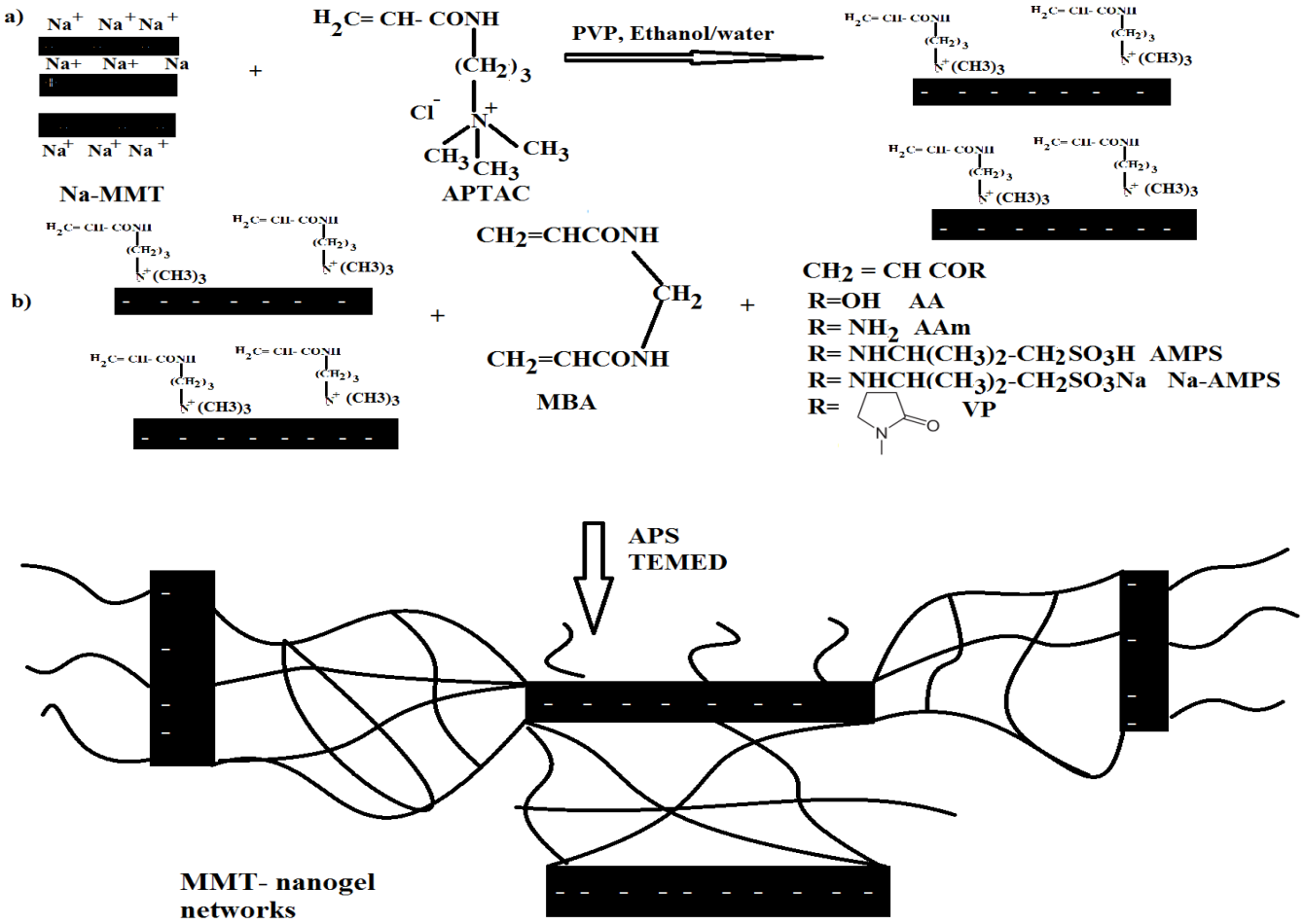

Scheme 1. Synthesis of MMT APTAC nanogels.

The crosslinked copolymers can form MMT nanopolymer composites through radical polymerization as described in the experimental section. It is expected that, the modification of Na-MMT with nanogel will change the surface properties and activity of MMT that was not reported elsewhere and will discuss in the next section.

3.1. Characterization of MMT nanogels:

The chemical structures of unmodified Na-MMT and modified nanogels with APTAC/Na-AMPS, APTAC/AMPS, APTAC/AA, APTAC/VP and APTAC/AAm are confirmed by FTIR analysis as represented in Fig. 1(a-f).

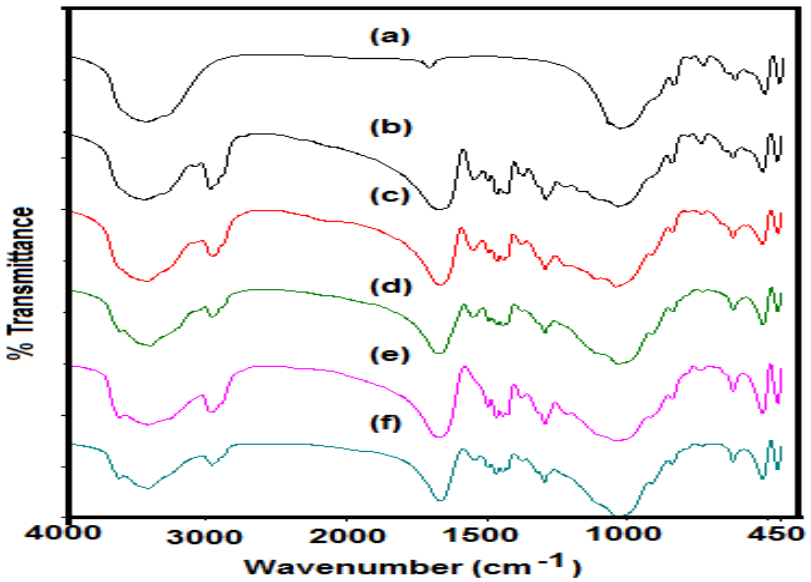

Figure 1. FTIR spectra of a) Na-MMT, b) MMT-APTAC/AMPS, c) MMT-APTAC/VP, d) MMT-APTAC/AAm, e) MMT-APTAC/Na-AMPS and f) MMT-APTAC/AA.

The data shows weakness and shift to lower wave number for characteristics of MMT bands at 3450 and 1645 cm^{-1} (Fig. 1a; referred to OH of water) after modification with nanogels. This behavior indicates that the amount of water is reduced by modification with nanogels and conversion of Na-MMT from hydrophilic to organophilic MMT. Moreover, all FTIR spectra, Fig.1a-f, confirm the appearance of bands Al(Mg)-OH (at 3630 and 795 cm^{-1}) , Si-O (at 1045 cm^{-1}) and Si-O-Si (at 920 and 845 cm^{-1}) [34]. The disappearance of =CH bands at 3000-3100 cm^{-1} (referred to Olefin CH stretching vibration) and appearance of bands at 2780 and 2985 cm^{-1} (represent CH_2 and CH_3 symmetric and asymmetric stretching vibration) elucidate the polymerization of monomers and modification of MMT with organic polymers. The appearance of absorption bands at 1690 and 1560 cm^{-1}, referred to CONH stretching vibration primary and secondary) indicates the formation of polymeric network based on APTAC/MBA and AAm, VP, AMPS, AA and Na-AMPS. These data propose that nanogel have modified at the surface or intercalate space of MMT.

The polymer contents and thermal stability of MMT nanogel can be confirmed by TGA-DTA analyses as represented in Fig. 2. The thermal analysis data at different temperatures and their residual at 650 ^{o}C were determined and listed in Table 1.

Table 1. TGA data of MMT-APTAC nanogels.

Weight loss (%)	Na-MMT	MMT nanogels				
		APTAC/Na-AMPS	APTAC/ AMPS	APTAC/AA	APTAC/AAm	APTAC/VP
25-200	5.5	2.8	3.2	2.9	4.2	3.5
200-550	-	48.2	65.1	47.3	57.0	61.5
550-750	3.5	4.0	4.0	4.0	5.3	3.5
Total	9	55.0	72.3	54.3	66.5	68.5

Careful inspection of the data listed in Table 1 and Fig.2 indicates that the mass losses from room temperature to 200 ^{o}C, correlated to water molecules bond with Na-MMT galleries, are reduced from 5.5 % to 2.8 t % which indicates the exchange of sodium cation with nanogel reduces the water bond to silicate OH groups of MMT layers [36].

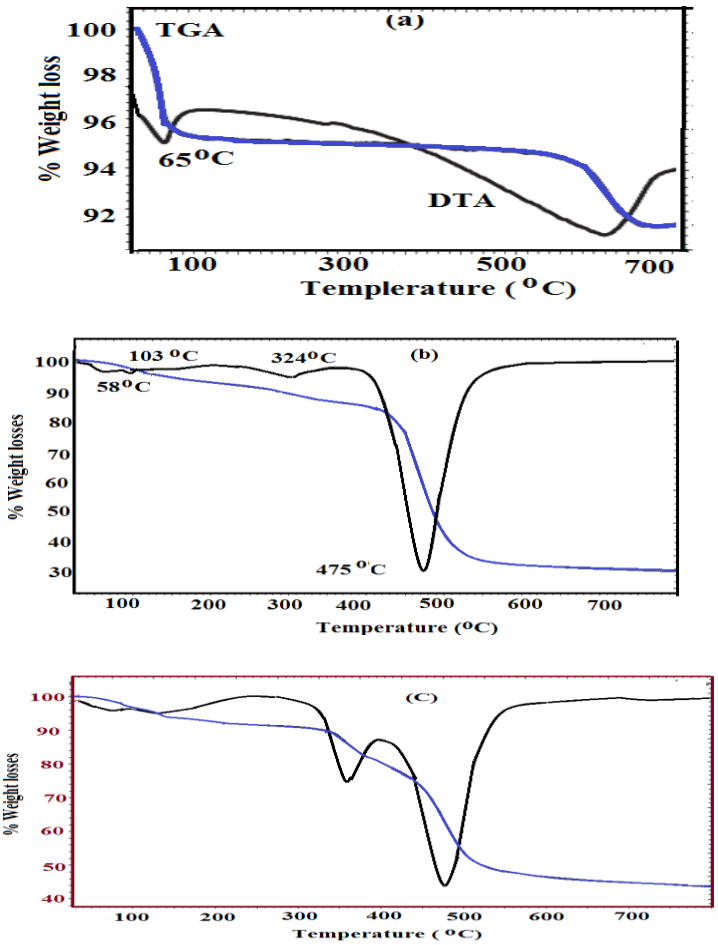

Figure 2. TGA and DTA thermograms of a)Na-MMT, b) MMT-APTAC/VP, and c) MMT-APTAC/Na-AMPS.

Moreover, the increment of weight loss percentages in the temperature range 200-550 ^{o}C by exchange of Na cation with cationic nanogels from 0 to more than 65.1 % , respectively confirm the incorporation of polymer network with MMT galleries. The DTA analysis indicates the appearance of exothermic peaks at 324 and 475 ^{o}C that confirm the decomposition of nanogel polymer composites. It was observed that the nanogel contents of polymer composites are reduced with incorporation of ionic monomers such as AMPS-Na and AA than nonionic such as VP and AAm. These data indicate that the repulsion between monomer negative charges and MMT negative charges (ionic monomers prevent the intercalation more nanogel among MMT galleries than nonionic monomer. The TGA data of APTAC/AMPS (Table 1) contradict this rule. Moreover, the data indicate that MMT modified with APTAC/AMPS losses 72.3 Wt. % more than other modified MMT nanogel composite. These data

suggest that, the combination between APTAC and AMPS as cationic and ionic polymers increase the intercalation of more polymers among the interlayer spaces of MMT.

It is well established that WAX is a useful technique to confirm the formation of nanocomposite, intercalation and exfoliation of Na-MMT [37-39]. In previous work [27, 28], the peak of Na-MMT appeared at 2-theta of 5.78^{o} (referred to 001 reflection plane, basal spacing 2.35 nm) is used to confirm the intercalation of MMT layers with organic polymers from change its position. Moreover, the disappearance of this peak confirms the exfoliation of MMT galleries [40]. In the present work, WAX analyses of MMT composites were represented in Fig.(3 a-e). The WAX (Fig. 3) indicates that MMT layers were exfoliated with APTAC/Na-AMPS, APTAC/AAm and APTAC/AMPS nanogels. Moreover, MMT layers are intercalated with APTA/AA and APTAC/VP due to shift of (001) peak to 4.7^{o} and 7 ^{o}, with basal plane 4.98 and 1.39 nm, respectively. The interaction between nanogel polymers is the main force to exfoliate or intercalate the MMT layers. These interactions are referred to van der Waals force between polymer skeleton chains or electrostatic interaction between the hydrophilic groups of polymers.

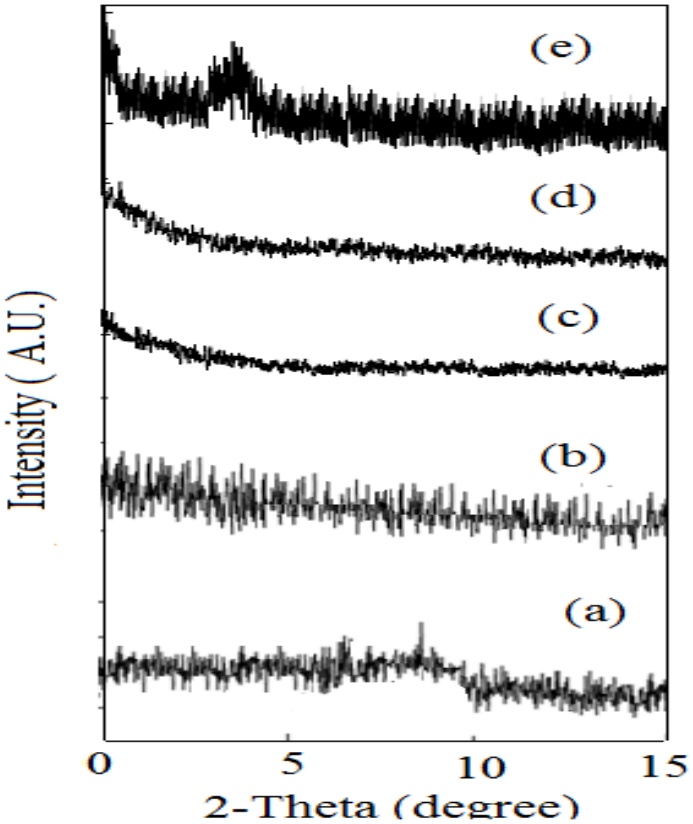

Figure 3. WAX diffractograms of a) MMT-APTAC/VP, b) MMT-APTAC/Na-AMPS, c) MMT-APTAC/Na-AAm, d) MMT-APTAC/AMPS and e) MMT-APTAC/AA.

The increment of intramolecular interactions between APTAC/VP amides arrange the polymer more closely into MMT galleries and reduce the basal space to 1.39 nm. Moreover, the repulsion

between APTAC/AA charges increases the interlayer space to 4.98 nm. These behaviors are observed for interaction MMT galleries with cationic and ionic surfactants [33, 41].

High resolution transmittance electron microscope (HR-TEM) is an effective tool to determine the exfoliation of nanocomposite materials [38, 42]. Hence, the TEM micrographs for selected MMT nanogels are represented in Fig. 4 a-d. The exfoliation of MMT galleries was observed for that modified with APTAC/AMPS and APTAC/Na-AMPS nanogels Fig. 4 a and d, respectively. The intercalations of MMT layers with APTAC/AAm, APTAC/AA and APTAC/VP, are detected Fig. 4 b –c. These mean that, the APTAC/AMPS and APTAC/Na-AMPS nanogels form elastic forces between MMT layers and assist to exfoliate MMT layers [43]. So, the copolymerization of APTAC with AA, VP and AAm does not produce elastic chains or particles to produce the forces required to exfoliate the MMT layers.

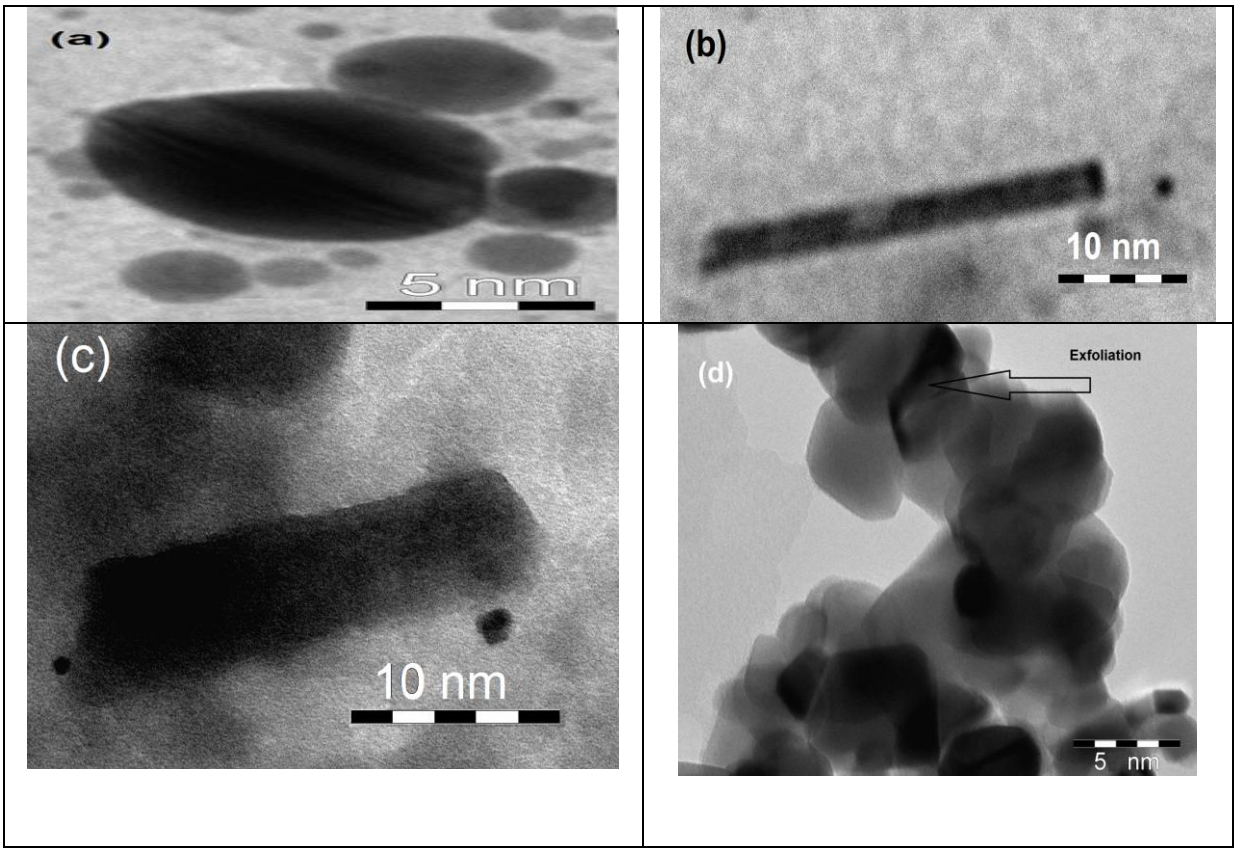

Figure 4. TEM micrographs of MMT modified with a) APTAC/AMPS, b) APTAC/AA, c) APTAC/AAm and d) APTAC/Na-AMPS nanogels.

Zeta potential is very important parameters that can be used to evaluate the the stability of colloidal systems of the MMT nanogel dispersion in water to increase their efficiencies in the removal of water pollutants. It is well known that the stable suspensions show zeta potential values higher than +30mV or lower than -30mV [44].Moreover, the negative charges on the surface of MMT nanogel is important for static interaction with cationic dye. Zeta potential data have been used to explain the

adsorption mechanisms of ionic moieties on the surface of MMT [45-48]. However, zeta measurements were conducted to determine the amount of MB required to neutralize the negative charge of clay. In this respect, zeta potential measurements are used to determine the charge of MMT nanogel composites as represented in Fig.5. The data indicate that the negative charges on the Na-MMT were reduced by forming dispersed MMT nanogels. The reduction of negative charges on MMT layers was referred to the exchange of Na cation with APTAC nanogels that intercalate or exfoliate MMT layers to equilibrate the negative charge density. The amide groups of VP and AAm act as neutral functional groups. The surface charges are the key factor for dispersability of MMT nanogel. It is well known that the particles possess small size and high surface charges with zeta potential more than 30 mV cannot combine to each other and have high dispersion stability in aqueous solution [49]. Accordingly, the ability of MMT nanogels to form hydrogen bonds with water is the main key factor for dispersability of MMT nanogels in water. The effect of pH on the zeta potential is investigated in 1mM of KCl solution at 25 ^{o}C. The increment of negative charges with increasing pH from 2 to 9 was refereed to ionization of ionic sulfonate and carboxylic groups of APTAC/Na-AMPS, APTAC/AMPS and APTAC/AA nanogels. Moreover deprotonation of amide groups increases the density negative charge on MMT layers with increasing pH of PBS from 2 to 9 [50].

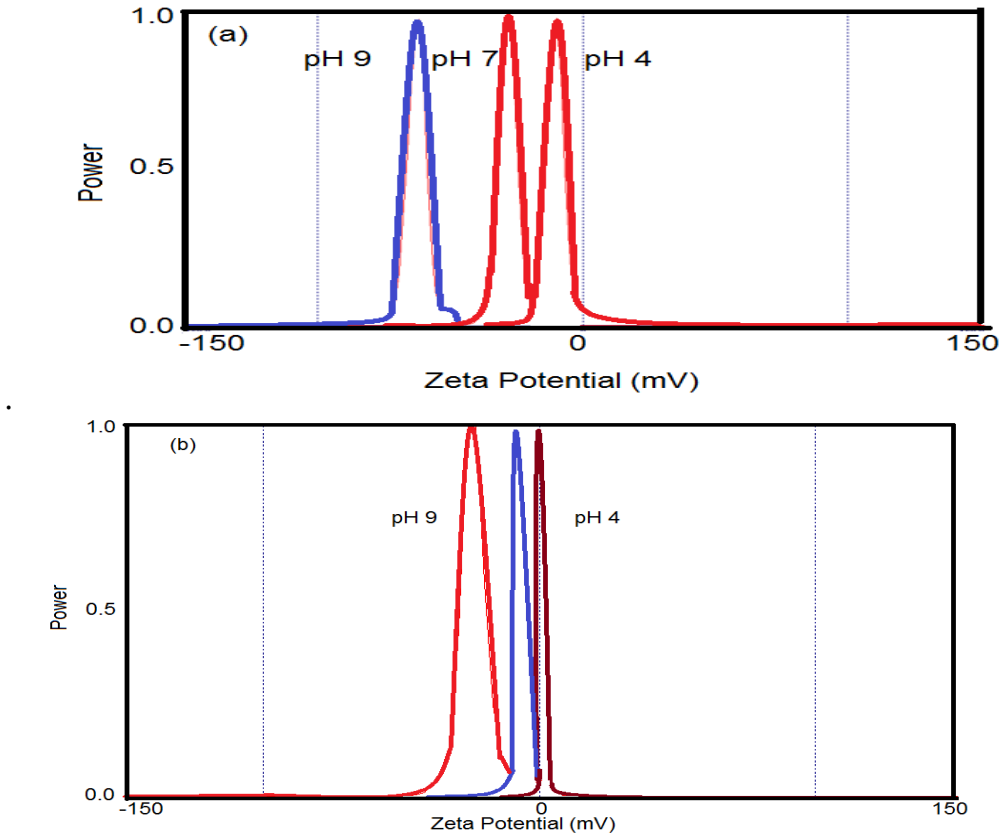

Figure 5. Zeta potential (mV) of a)Na-MMT and b) MMT-APTAC/AA in aqueous 0.01 M of KCl and different pH at 25 ^{o}C.

3.2. Surface Properties of MMT nanogels

The presence of functional groups such as quaternary trimethyl ammonium, amide, carboxylic acid and sulfonic acid will affect the intra- and intermolecular interactions between nanogels and water. The increasing of interactions between water and MMT nanogel composites will reflect on their surface activity or on the ability of MMT nanocomposites to reduce the surface tension of water. So that, the relation between the surfaces tension of water (γ; mN/m) and concentrations of MMT nanogel composites (ln c; mol/L) was represented in Fig. 6.

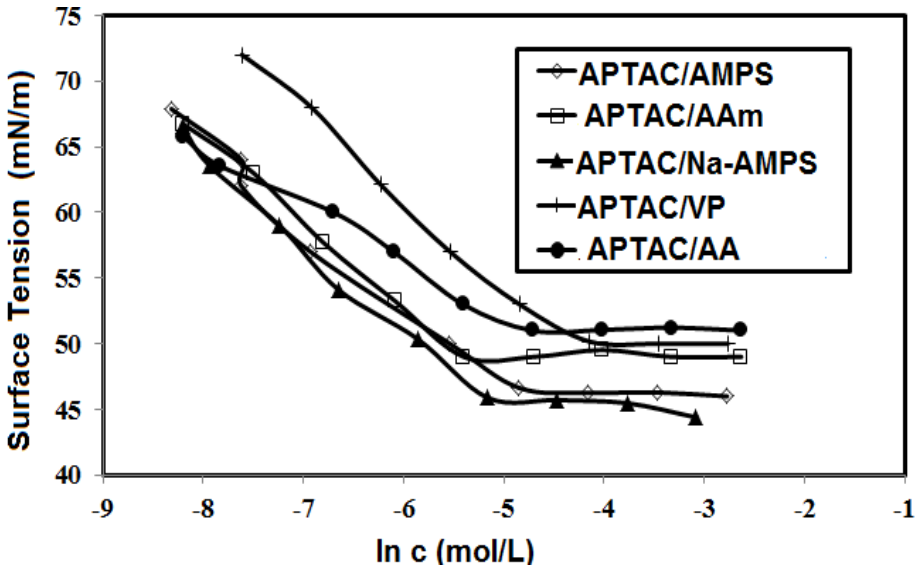

Figure 6. Relation between surface tension of water and concentrations of MMT nanogels at 25 ^{o}C.

Table 2. Surface activity parameters of amphiphilic MMT nanogels in water at 25^{o}C.

MMT Nanogels modifier	cmc mol/L x 10^3	γ_{cmc} mN/m	$\Delta\gamma = \gamma_{o-}\gamma_{\pi cmc}$ mN/m	$(-\partial\gamma / \partial \ln c)$	Γ_{max} x 10^{10} mol/ cm^2	A_{min} nm^2/ molecule	-ΔG kJmol^{-1}	
							ΔG_{agg}	ΔG_{ads}
APTAC/Na-AMPS	5.7	44.1	28.0	10.9	4.5	0.37	12.31	18.53
APTAC/AMPS	7.8	46.1	26.0	9.3	3.9	0.43	11.57	18.28
APTAC/AA	8.9	51.1	21.0	4.8	2.0	0.83	11.26	21.72
APTAC/AAm	4.5	49.1	23.0	7.9	3.3	0.51	12.88	19.92
APTAC/VP	15.8	50.1	22.0	5.9	2.5	0.66	9.89	18.60

The data of Fig. 6 indicates that the surface tension of water is reduced with increasing the concentrations of MMT nanogel composites to definite concentrations. The γ values are not reduced above these concentrations which named as critical aggregation concentrations (cac; mol/L). The values of cac are determined and listed in Table 2. The cac of MMT nanogel composites indicates that these composites behave as surfactants to adsorb at interface or aggregate in bulk solutions.

The enhancement of intermolecular interactions between MMT nanogel composites due to electrostatic attraction will increase the aggregation of MMT nanogel composites in water solution. Moreover, the interactions between water and MMT nanogel composites through repulsion between ionic groups and formation of strong hydrogen bonds between water and MMT nanogel composites will increase the adsorption and dispersion of nanogels in water. The values of MMT nanogel composites cac are arranged in the order APTAC/VP>APTAC/AA> APTAC/AMPS > APTAC/Na-AMPS > APTAC/AAm. While the surface tension values at cac, γ_{cac}, listed in Table 2 confirm that the ability of MMT nanogel to reduce the water surface tension are ordered as: APTAC/Na-AMPS > APTAC/AMPS > APTAC/AAm > APTAC/VP > APTAC/AA. These data indicate that the exfoliation of MMT layers plays an important role to increase the surface activity of MMT nanogel composites to be more effective at lower concentrations (cac). These data was in agreement with the zeta potentials and WXD data. The zeta potential data (Figure 5) show that the MMT surface is modified by the adsorption of copolymer nanogels in a manner best explained by molecular charges related to the cation exchanges of Na cation with nanogels. Consequently, the surface properties of the solid/liquid show additional differences among the copolymer nanogels that may influence their interactions with water. For solid–liquid systems, the zeta potential confirms the electrical potential that will change the adsorption of highly charged anionic species such as nanogels [51-53], and may influence the subsequent binding of charged molecules and their interaction with water. The observed differences in zeta potentials and surface tension are likely to contribute to the application of MMT nanogel composites as adsorbent in aqueous system. These properties, therefore, have affected the adsorption and diffusion of pollutants on the surface of MMT nanocomposite. These charges on MMT may affect their ability to attract other ions, or charged substances and macromolecules. In other words, the adsorption capacity of any adsorbents may vary as a result of zeta potential and their interaction with water.

The concentrations of MMT nanogel composites at the air/ water interface can be determined from slope of linear plot between γ and ln c ($-\partial \gamma / \partial \ln c$), surface excess concentrations (Γ_{max}) and area per molecules $A_{min.}$ These parameters are calculated according to our previous publications [54-57] and listed in Table 2. The data indicates that the surface activity of MMT nanogel composite is arranged as APTAC/Na-AMPS> APTAC/AMPS> APTAC/AAm> APTAC/VP> APTAC/AA that reflects on their affinity to adsorb at the air/water interface. Moreover, the increment of surface activity and Γ_{max} is reflected on the packing degree and arrangements of solid particles at the interface [58, 59]. This means that the exfoliations of MMT increase the ordering and interaction of hydrophilic part in the water and hydrophobic parts in the air at an interface that increases the Γ_{max}. The intercalation of MMT with APTAC/VP and APTAC/AA reduces Γ_{max} and increases A_{min} due to the growing of repulsive forces between MMT layers at the interface which confirms the disordering packing of nanogels at the air/water interface. The ability of amphiphilic MMT nanogels to favor the

aggregation or adsorptions can be determined from the free energy of aggregation and adsorption ΔG_{agg} and ΔG_{ads} that calculated as discussed in previous work [54-57] and listed in Table 2. The values of ΔG_{ads} are greater than ΔG_{agg} which confirms that the adsorption of the MMT nanogels at interfaces is preferred at interfaces more than aggregation. Moreover, ΔG_{ad} values are more negative than ΔG_{agg}, confirming that the adsorption of MMT nanogels at interfaces decreases the free energy of the system. The high surface activity and lowering of free energy of the system produced from the interaction of MMT nanogels with water have supported the application of these nanocomposites in the field of water treatment as adsorbents for toxic organic materials.

3.3. Removal of MB dye pollutant

There are three alternative mechanisms reported to explain the efficiency of adsorbents to remove toxic cationic pollutants such as dyes and heavy metals from water [60]. The electrostatic interactions and dipole-dipole interaction mechanisms between charges are preferred mechanism for anionic adsorbents and pollutants more than chemical interactions. In this work, the adsorption of MB as cationic dye is investigated using MMT nanogels. The adsorption isotherm is studied using Langmuir [61] or Freundlich [62] as illustrated in equations 3 and 4:

$$(C_e/Q_e) = [(1/Q_{max}\, K_l) + (C_e/Q_{max})] \quad (3)$$

$$\log (Q_e) = \log (K_f) + [(1/n) \times \log (C_e)] \quad (4)$$

where Q_e, Q_0, C_e, n, K_l and K_f are the equilibrium and maximum amount of dye (mg/g) adsorbed on MMT nanogel composites, the concentration of dye solution at equilibrium (mg/L), empirical constant , Langmuir and Freundlich constants, respectively.

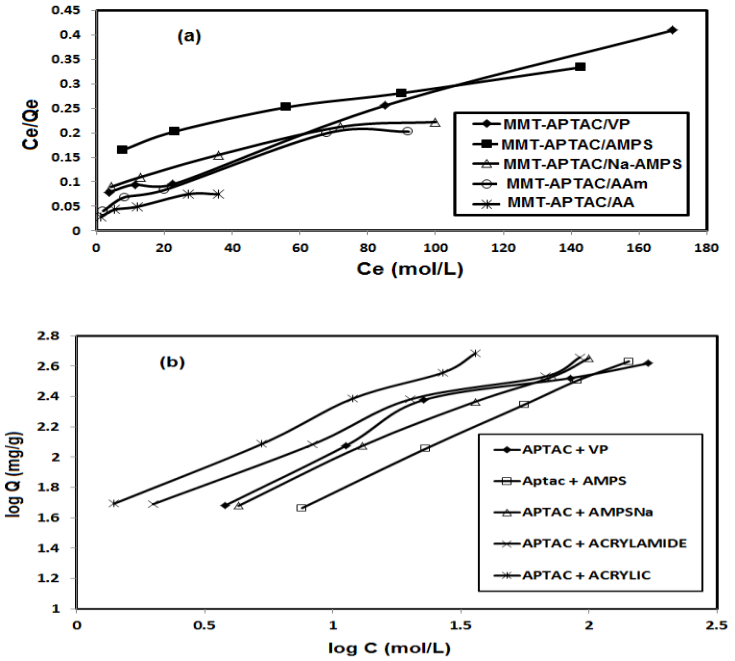

Figure 7. MB adsorption isotherms of a) Langmuir and b) Freundlich plots using MMT nanogels.

The 1/n values are used to investigate the adsorption intensity of MB dye onto MMT nanogel. The relations of C_e/Q_e against C_e and ln Q_e versus ln C_e are represented in Fig. 7. The Langmuir and Freundlich constants are determined and listed with the experimental Q_{max} and % E in Table 3. The linear adsorption isotherms obey Langmuir model and achieve good regression coefficients R^2 than that of the Freundlich model.

The linear plots of Langmuir confirm the formation of monolayer of adsorbate (MB) on the active site of MMT layers. Moreover, the appearance of the S curve indicates that the MB molecule has a moderate degree of intermolecular attraction with MMT nanogel that causes their molecules to pack vertical as adsorbed or these molecules compete with solvent molecule to interact with MMT nanogels [**63**]. This means that the adsorption of water layers to cover the MMT nanogels, however, the interactions between MB molecules with MMT nanogels will decrease and affect the dispersion energy of water with the dye. Consequently, a type-S isotherm will produce to confirm the heterogeneity of MB adsorption as the formation of multilayer on some of the MMT nanogel surface, while the monolayer is still incomplete on another site of MMT nanogel parts. The S- curves are appearing in MMT-APTAC/AA and MMT-APTAC/VP which possess low surface activity to reduce the water surface tension (Table 1) that proves the lower dispersion of MB into MMT nanogel layers. The zeta potential data (Figure 4) confirms that the MMT nanogel have more negative charges in basic medium and consequently the interaction between MB cations and MMT negative charges increased at pH 9 more than other pHs. This data confirm the effect of zeta potential on the adsorption of charged dyes on the surface of charges adsorbents.

Table 3. Adsorption isotherm parameters for removal of 1000 ppm of MB dye using amphiphilic Na-MMT nanogels at 25 ^oC.

Adsorbents	Langmuir isotherm parameters			Freundlich isotherm parameters			Exp. Adsorption capacity at 1000 ppm	
	Q_{max} mg/g	K_l L/mg	R^2	1/n	K_f	R^2	Q_{max} mg/g	% E
Na-MMT	344.3	0.027	0.9817	0.686	0.049	0.906	310	82
APTAC/Na-AMPS	714.3	0.043	0.9828	0.694	0.1023	0.995	850	99.5
APTAC/AMPS	833.3	0.007	0.9897	0.763	0.0015	0.998	720	99.1
APTAC/AA	769.2	0.040	0.9747	0.695	0.203	0.995	551	92.23
APTAC/AAm	526.3	0.040	0.985	0.562	0.193	0.979	428	85.7
APTAC/VP	476	0.032	0.993	0.550	0.167	0.922	415	83

The effect of contact times on Q values for removal of MB from water at pH 7 are illustrated in Fig. 8. The data indicate that the MB was removed from water during time ranged from 20 to 60 minutes. The ability of MMT nanogels to remove MB is arranged in the order: APTAC/Na-AMPS>

APTAC/AMPS> APTAC/AAm> APTAC/VP> APTAC/AA; which resemble to the order surface activity that discussed in the previous order.

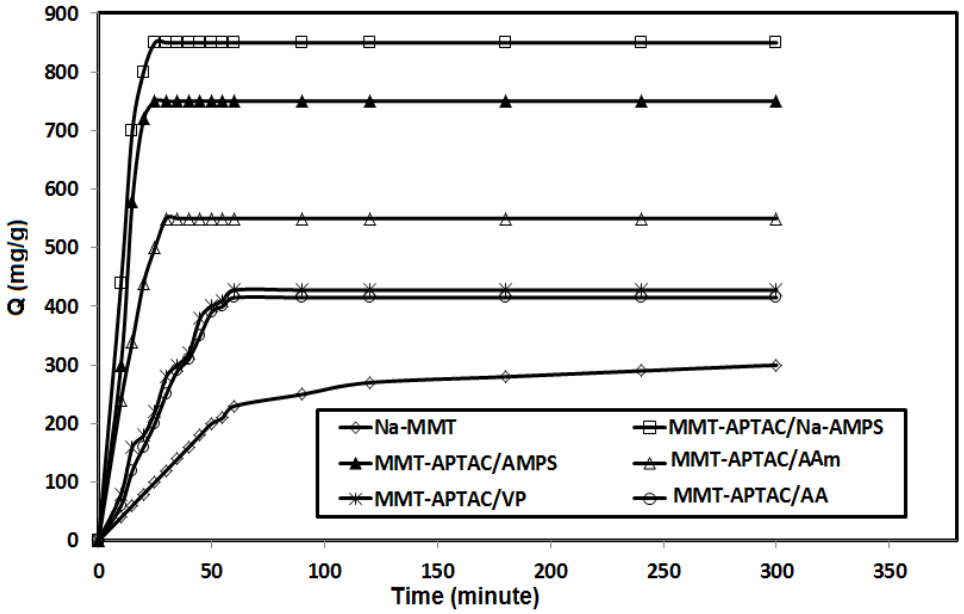

Figure 8. Effect of time on MB removal using MMT nanogels at 25 ^{o}C and pH 7.

This means that the ability of MMT nanogels to reduce the surface tension is the main factor to increase MB diffusion onto MMT layers. Moreover, the high adsorption efficiency is obtained during the first ten minutes (60-75 %) and then increased gradually to achieve the maximum during times ranged from 10-40 minutes.

The MMT- nanogels were de-swelled and reused as described in the experimental section. The data indicate that the efficiencies of MMT nanogels to remove MB are stable and decreased after three cycles from 1-3 %. These results show the high efficiency of MMT nanogels to reuse different times from point of economic view.

4. CONCLUSIONS

In conclusion, the crosslinking copolymerization technique of APTAC with AMPS, AMPS-Na and AAm exchanged Na cation and exfoliate Na-MMT to produce amphiphilic MMT nanogels. The complete exfoliation of MMT nanomaterials reduced the surface tension of water. The order of reduction of water surface tension increased in the order APTAC/Na-AMPS> APTAC/AMPS> APTAC/AAm> APTAC/VP> APTAC/AA nanogel. The zeta potential data described here reveal the differing abilities of MMT nanogels to adsorb the MB cationic dye on their surfaces. The observed differences in zeta potential data of MMT nanogel will influence the rate and extent of binding affinities and in effects on their surface properties. The MMT nanogels showed high efficiency to remove MB from water during 20 minutes. The dipole-dipole interaction mechanism is used to explain

the MB removal from water. The differences zeta potential and surface tension of MMT nanogels are consistent with the determined MB removal efficiencies to conclude that they likely affect the diffusion of dye into the nanogel networks.

ACKNOWLEDGEMENT
The authors extend their appreciation to the Deanship of Scientific Research at King Saud University for funding this work through research group no RGP-VPP-235.

References

1. S. Daer, J. Kharraz, A. Giwa, S.W. Hasan, *Desalination*, 367 (2015) 37-48.
2. H. M. Hegab, L. Zou, *Journal of Membrane Science*, 484 (2015) 95-106.
3. H. Dong, L. Zhao, L. Zhang, H. Chen, C. Gao, W.S. Winston Ho, *Journal of Membrane Science*, 476 (2015) 373-383.
4. C. Luo, J. Wang, P. Jia, Y. Liu, J. An, B. Cao, K. Pan, *Chemical Engineering Journal*, 262 (2015) 775-784.
5. S.T. Mostafavi, M.R. Mehrnia, A.M. Rashid, *Desalination*, 238 (2009) 271-280.
6. D. H. K. Reddy, S-Mok Lee, *Advances in Colloid and Interface Science*, 201–202 (2013) 68-93.
7. G. Bringmann, R. Kühn, *Water Research*, 14(1980) 231-241.
8. US Environmental Protection Agency official website hhttp:// www.epa.govi.
9. M. S. Bootharaju and T. Pradeep, *J. Phys. Chem*. C 2010, 114, 8328–8336.
10. K. Jayaraman, *Chem. World* 4 (2007) 15–15.
11. J. Guo, X. Cai, Y. Li, R. Zhai, S. Zhou, Ping Na, *Chemical Engineering J*. 221 (2013) 342-352.
12. S. Syed, M.I. Alhazzaa, M. Asif, *Chemical Engineering Journal*, 167(2011) 99-103.
13. R.A. Crane, T.B. Scott, *Journal of Hazardous Materials*, 211–212(2012) 112-125.
14. O. Kammona, E. Dini, C. Kiparissides, R. Allabashi, *Microporous and Mesoporous Materials* 110
15. M. A. Akl, A. A. Sarhan, K. R. Shoueir, A. M. Atta, *Journal of Dispersion Science and Technology*, 34(2013)1399–1408.
16. A. M. Atta, H.S. Ismail, A. M. Elsaaed, *Journal of Applied Polymer Science*, 123 (2012) 2500–2510.
17. J. Gregoryb, *Water Research* 41 (2007) 2301 – 2324
18. E. González-Pradas, M. Villafranca-Sánchez, A. Gallego-Campo, D. Ureña-Amate , M. Fernández-Pérez, *J. Chem. Technol. Biotechnol*. 74 (1999) 49-54.
19. P. Fruhstorfer, R.J. Schneider, L.Weil, R. Niessner, *Science of the Total Environment* 138 (1993) 317-328.
20. E. González-Pradas, A. Valverde-Garc, M. Villafranca-Sánchez, *J. Chem. Technol. Biotechnol*.47(1990)15-22.
21. R. Bhattacharyya, S. K. Ray, *Chemical Engineering Journal*, 260 (2015) 269-283.
22. Y. Zhao, E. Abdullayev, A. Vasiliev, Y. Lvov, *Journal of Colloid and Interface Science*, 406 (2013) 121-129.
23. I. Larraza, M. López-Gónzalez, T.Corrales, G. Marcelo, *Journal of Colloid and Interface Science*, 385 (2012) 24-33.
24. X. Nie, A. Adalati, J. Du, H. Liu, S. Xu, J. Wang, *Applied Clay Science*, 97–98 (2014) 132-137.
25. C.W. Chiu, C.C. Chu, W.T. Cheng, J.J. Lin, *European Polymer Journal*, 44 (2008) 628-636.
26. L. Liang, J. Liu, X. Gong, *Langmuir*, 16 (2000) 9895-9899.
27. A. M. Atta, G. A. El-Mahdy, H. A. Al-Lohedan, A. M. Tawfeek, A. A. Abdel-Khalek , Digest *Journal of Nanomaterials and Biostructures*. 9 (2014) 531 – 541.

28. A.M. Atta, G.A. El-Mahdy, H.A. Al-Lohedan, A.M. Tawfeek, S. R. Sayed, *Int. J. Electrochem. Sci.*, 10(2015)2377-2390.
29. S.A. Boyd, M.M. Mortland, C.T. Chiou, *Soil Sci. Soc. Am*. J. 52 (1998) 652–657.
30. J.A. Smith, P.R. Jaffe, C.T. Chiou, *Environ. Sci. Technol*. 24 (1990) 1167–1172.
31. A.S. Ozcan, E. Bilge, A. Ozcan, *J. Colloid Interface Sci*. 280 (2004) 44–54.
32. M. Akcay, *J. Colloid Interface Sci*. 280 (2004) 299–304.
33. D. Chen, J. Chen, X. Luan, H. Ji, Z. Xia, *Chemical Engineering Journal* 171 (2011) 1150– 1158.
34. S.A. Boyd, G. Sheng, B.J. Teppen, C.T. Johnston, *Environ. Sci. Technol*. 35 (2001) 4227–4234.
35. D.W. Rutherford, C.T. Chiou, *Environ. Sci. Technol*. 26 (1992) 965–970.
36. W. Xie, R.C. Xie, W.P. Pan, D. Hunter, B. Koene, L.S. Tan, R. Vaia, *Chem. Mater*. 14 (2002) 4837–4845.
37. N. Greesh, P. C. Hartmann, V. Cloete, R. D. Sanderson, *Journal of Colloid and Interface Science* 319 (2008) 2–11.
38. K. Kabiri, H. Mirzadeh, M. J Zohuriaan-Mehra, M. Daliri, *Polym Int* 58 (2009) 1252–1259.
39. L. Liang, J. Liu, X. Gong, *Langmuir*, 16 (2000) 9895-9899.
40. F. Piscitelli, P. Posocco, R. Toth, M. Fermeglia, S. Pricl, G. Mensitieri, M. Lavorgn, *Journal of Colloid and Interface Science*, 351 (2010) 108
41. H. Mao, B. Li, X. Li, L. Yue, Z. Liu, W. Ma, *Ind. Eng. Chem. Res*. 49 (2010) 583–591.
42. K.C. Chang, S.T. Chen, H.F. Lin, C.Y. Lin, H. Huang, J. M. Yeh, Y. H. Yu, *European Polymer Journal* 44 (2008) 13–23.
43. J.H. Park, S.C. Jana, *Macromolecules* 36 (2003) 2758-2768.
44. H. Sun, J. Yu, P. Gong, D. Xu, C. Zhang, S. Yao, *Journal of Magnetism and Magnetic Materials* 294 (2005) 273–280.
45. S. Tunç, D. Osman, B. Kanci, *Colloid Surf. A* 398 (2012) 37-47.
46. S. Xu, S.A. Boyd, *Langmuir* 11 (1995) 2508-2514.
47. P. Somasudaran, D.W. Fuerstenau, *J. Phys. Chem*. 70 (1966) 90-96.
48. Y. Yamaguchi, H. Hoffmann, *Colloids and Surf. A* 121 (1997) 67-80.
49. P. Somasudaran, T.W. Healy, D.W. Fuerstenau, *J. Phys. Chem*. 68 (1964) 3562-3566.
50. K. M. Ho, P. Li, *Langmuir*, , 24(2008) 1801-1807.
51. O. Sahin, A.N. Bulutcu, *Cryst. Res. Technol.* 38(2003 56–62.
52. L.C. Cao, G. Deng, E.R. Boeve, W.C. de Bruijn, R. de Water, C.F. Verkoelen, J.C. Romijn, F.H. Schröder, *Scanning Microsc.* 10 (1996 401–414.
53. G.H. Nancollas, W.Wu, *J. Dispersion Sci. Technol.* 19 (1998) 723–738.
54. A. M Atta, *Polym Int* 63(2014) 607–615.
55. A. M. Attaa, A. K. F. Dyaba, H. A. Allohedan, *Polym. Adv. Technol*., 24(2013) 986–996.
56. A. M. Atta, A. K. F. Dyab, H. A. Al-Lohedan, *J Surfact. Deterg*. 16(2013) 343–355.
57. A. M. Atta, A. K. F. Dyab, H. A. Al-Lohedan, K. A. AlJenady, *Polymer Science B*, 56 (2014) 770-787.
58. B.P. Binks, P.D.I. Fletcher, S.N. Kotsev, *Langmuir* 13 (1997) 6669–6682.
59. B.P. Binks, P.D.I. Fletcher, W.F.C. Sager, *J. Mol. Liq.* 72 (1997) 177–190.
60. G. Rytwo, D.Tropp, C.Serban, *Appl. Clay Sci*. 20 (2002)273–82.
61. I. Langmuir, *J. Am. Chem. Soc*. 40(1918)1361–1403.
62. Freundlich HMF. Z. *Phys. Chem*. 57(1906) 385–470.
63. C.H Giles, A.P D'Silva, I. Easton, *J. Coll. Interface Sci*. 47(1974)766-778.